Talanta 127 (2014) 255–261

Contents lists available at ScienceDirect

Talanta

journal homepage: www.elsevier.com/locate/talanta

An electrochemical sensor for simultaneous determination of ascorbic acid, dopamine, uric acid and tryptophan based on MWNTs bridged mesocellular graphene foam nanocomposite

Huixiang Li, Yi Wang, Daixin Ye, Juan Luo, Biquan Su, Song Zhang, Jilie Kong *

Department of Chemistry, Fudan University, Shanghai 200433, PR China

ARTICLE INFO

Article history:
Received 3 December 2013
Received in revised form
11 March 2014
Accepted 13 March 2014
Available online 21 March 2014

Keywords:
Multi-walled carbon nanotubes
Mesocellular graphene foam
Ascorbic acid
Dopamine
Uric acid
Tryptophan

ABSTRACT

A multi-walled carbon nanotubes (MWNTs) bridged mesocellular graphene foam (MGF) nanocomposite (MWNTs/MGF) modified glassy carbon electrode was fabricated and successfully used for simultaneous determination of ascorbic acid (AA), dopamine (DA), uric acid (UA) and tryptophan (TRP). Comparing with pure MGF, MWNTs or MWNTs/GS (graphene sheets), MWNTs/MGF displayed higher catalytic activity and selectivity toward the oxidation of AA, DA, UA and TRP. Under the optimal conditions, MWCNs/MGF/GCE can simultaneously detect AA, DA, UA and TRP with high selectivity and sensitivity. The detection limits were 18.28 μmol L^{-1}, 0.06 μmol L^{-1}, 0.93 μmol L^{-1} and 0.87 μmol L^{-1}, respectively. Moreover, the modified electrode exhibited excellent stability and reproducibility.

1. Introduction

Ascorbic acid (AA), dopamine (DA), uric acid (UA) and tryptophan (TRP) play vital roles in physiological function of organisms [1–3]. AA is not only very popular for its antioxidant properties, but also used for the prevention and treatment of the common cold, mental illnesses, infertility, cancers and AIDs [4,5]. DA is a natural neurotransmitter which plays important roles in control of central nervous system, cardiovascular, renal, and hormonal functions. As well, it is involved in drug addiction and in Parkinson's disease [6–8]. UA is also an important biomolecule existing in blood and urine. Several diseases, such as gout, hyperuricaemia, and Lesch–Nyhan syndrome are related with the extreme abnormalities of UA levels [9,10]. As an essential amino acid, Trp is important in the maintenance of muscle mass and body weight in humans [11]. It has been implicated as a possible cause of schizophrenia in people who cannot metabolize it properly [12]. These small biomolecules usually coexist in biological matrixes [13,14]. Therefore, the simultaneous determination of them plays an important role in the field of biomedical chemistry, neurochemistry and diagnostic research. As AA, DA, UA and TRP are electroactive, electrochemical techniques arise great interest for their rapid response, high sensitivity, simple operation and low cost. However, at a bare electrode, the direct redox reactions are irreversible and the oxidation potential of these analysts is close enough to make their voltammetric responses overlap [15]. So the simultaneous determination on a bare electrode is impossible and the modification of electrode is necessary. A variety of materials have been used for the modification of electrode, such as gold nanoparticles/overoxidized-polyimidazole composite [16], graphene hybrid tube-like structure [13] and iron ion-doped natrolite zeolite–multiwall carbon nanotube [17].

As possessing high electrical conductivity, larger specific surface area, and chemical stability, MWNTs and graphene sheets (GS) have also been widely used as excellent matrixes on the electrodes for the analysis of AA, DA, UA or TRP, such as anthanum–MWNT nanocomposites for simultaneous determination of AA, DA, UA and nitrite [18], non-covalent iron(III)–porphyrin functionalized MWNTs for the simultaneous determination of AA, DA, UA and nitrite [19], poly(orthanilic acid)–MWNTs composite film-modified glassy carbon electrode (GCE) for the simultaneous determination of UA and DA in the presence of AA [20], MWNT modified carbon-ceramic electrode for simultaneous determination of AA, DA and UA [21]. Chen et al. built a DA sensor based on a GCE modified with a reduced graphene oxide and palladium nanoparticles composite, and the electrode can oxidize DA at lower potential [22]. Yang et al. constructed a highly sensitive and selective DA biosensor based on 3, 4, 9, 10-perylene tetracarboxylic acid functionalized GS/MWNTs/

* Corresponding author. Tel.: +86 21 65642138; fax: +86 21 65641740.
E-mail address: jlkong@fudan.edu.cn (J. Kong).

http://dx.doi.org/10.1016/j.talanta.2014.03.034
0039-9140/

IL composite film modified electrode [23]. Graphene is a single-atom thick, two-dimensional material that has attracted great attention due to its remarkable electronic, mechanical, and thermal properties since it was first reported in 2004 [24]. Although satisfied results were obtained in above studies, the nanocomposites based GS are complicate or time consuming to prepare since GS tends to form irreversible agglomerates or even restack to form graphite through van der Waals interactions. So, it was expected to obtain a kind of graphene where sheets were separated from each other and thus the agglomerates were avoided.

Herein, with the aim of simultaneous detection of AA, DA, UA and TRP, a facile and effective method using MWNTs bridged mesocellular graphene foam (MWNTs/MGF) as electrode material was put forward. This strategy was provided with following advantages. Firstly, MGF obtained by templated synthesis solved the problems such as conglomeration and uncontrollable dimensions because there were certain spaces among sheets [25]. Secondly, MWNTs were bridged to MGF via π–π stacking interaction to form loose and porous three-dimensional structures, which not only increased the surface areas but enhanced electrical conductivity. Therefore, MWNTs/MGF/GCE may be used for the simultaneous determination of AA, DA, UA and TRP.

2. Experimental

2.1. Reagents and chemicals

DA, UA and Trp were purchased from Sigma. AA was purchased from Sinopharm Chemical Reagent Co., Ltd. AA, DA, UA and Trp solutions were prepared fresh prior to use. Phosphate buffer solutions (PBS) (0.1 mol L^{-1}) at various pH were prepared using 0.1 mol L^{-1} Na_2HPO_4, 0.1 mol L^{-1} KH_2PO_4 and 0.1 mol L^{-1} KCl. Multi-walled carbon nanotubes (MWNTs) were purchased from Shenzhen Nanotech Port Co. Ltd. (diameter: 10–30 nm, length: 0.5–40 μm, Shenzhen, China). Other reagents were of analytical grade and used as received. All water used was twice distilled. All the measurements were performed at room temperature.

2.2. Apparatus

All electrochemical experiments including cyclic voltammetry (CV) and differential pulse voltammetry (DPV) were carried out on a CHI 1030 multichannel voltammetric analyzer (CH Instruments, Chenhua Corp., Shanghai, China). Electrochemical impedance spectroscopy (EIS) was carried out on an Autolab PGSTST 30 analyzer (Metrohm Autolab B.V., Switzerland). The conventional three-electrode system was employed with a platinum wire as the counter electrode, a saturated calomel electrode (SCE) as the reference electrode, and a bare GCE (Φ=3 mm) or modified electrode as working electrode. The surface morphology of electrode was observed by scanning electron microscopy (SEM) using a Philips XL30 Microscope (Japan).

2.3. Preparation of graphene based nanomaterial

MGF was easily synthesized in large amounts by using zeolite Ni-MCM-22 as a catalyst and template according to the method reported by our group [25]. As for control, GS obtained from chemical reduction was also prepared according to literature [26]. MWNTs were purified according to the method described in literature [27]. The MWNTs/MGF nanocomposite was prepared by dispersing 1 mg resulting MWNTs and 1 mg MGF in 1 mL *N*, *N*-dimethyl formamide (DMF) in the aid of ultrasonic agitation. For comparison, MWNTs suspension, MGF suspension and MWNTs/GS suspension were also prepared under the same conditions.

2.4. Preparation of modified electrodes

The bare GCE was first polished to a mirror-like surface with 0.3 and 0.05 μm α-alumina slurry, then rinsed and ultrasonicated sequentially in water, ethanol, diluted HNO_3 and water. Finally, it was dried under the stream of high purity nitrogen for further use.

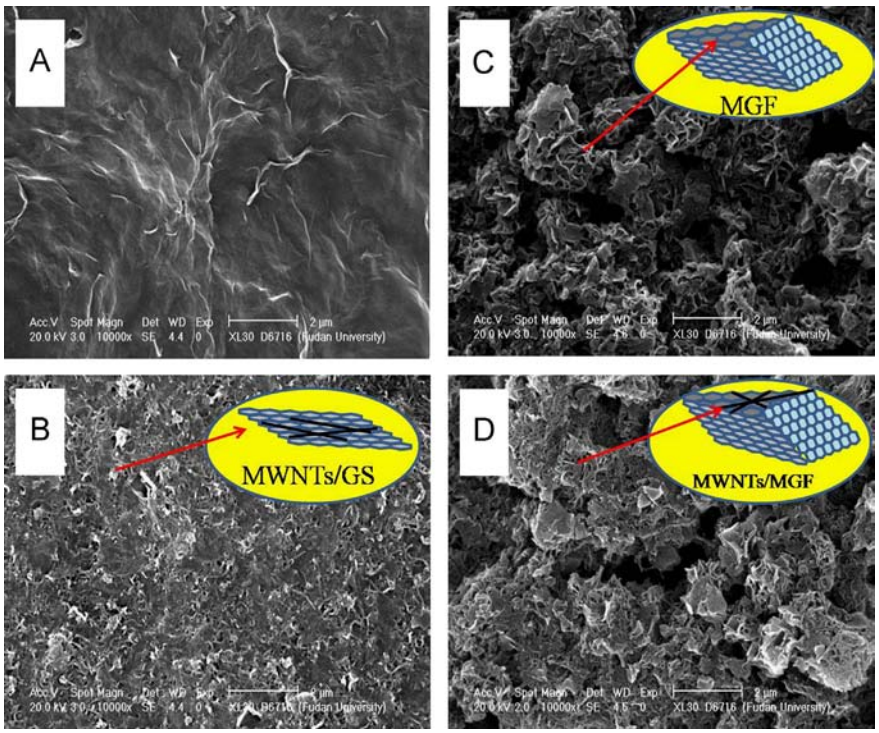

Fig. 1. SEM images of (a) GS, (b) MWNTs/GS, (c) MGF and (d) MWNTs/MGF. Inset: diagram of corresponding materials.

1 μL of the above-mentioned suspensions was casted on the surface of the clean GCE. The modified electrode was dried under an infrared lamp and rinsed with distilled water prior to use.

3. Results and discussion

3.1. SEM characterization of nanocomposite materials

The morphologies and microstructures of GS, MGF, MWNTs/GS, and MWNTs/MGF were investigated by using SEM (Fig. 1). Fig. 1a displays the SEM of GS synthesized by chemical reduction of graphene oxide. When it was ultrasonicated with MWNTs, MWNTs laid on the surface of GS forming simple and uniform accumulation which is shown in Fig. 1b. Fig. 1c is the SEM of MGF in which graphene sheets supported each other to form porous and foam-like stereoscopic architecture. When MGF were mixed under ultrasonication with MWNTs, MWNTs seeming as bridges suspended among graphene sheets to form loose and porous structures which are shown in Fig. 1d. The bridged state was observed obviously by the comparison of diagrams inserted in Fig. 1b and d. Compared with the compact compositions of MWNTs/GS, MWNTs bridged MGF possessed larger surface area.

3.2. Electrical responses of AA, DA, UA and TRP at modified electrode

Fig. 2 shows the differential pulse voltammograms (DPV) of different modified electrodes in 0.1 mol L^{-1} PBS (pH=7.3) containing the mixture of AA, DA, UA and TRP. At the bare GCE, the peaks for AA and DA overlapped together and came into one peak. What is more, the peak current was too small to get enough sensitivity. Consequently, it is difficult to detect the four small biomolecules simultaneously at bare GCE. When MWNTs or MGF was modified to the surface of GCE, peak current was improved obviously and the differences between their peak potentials were larger. Especially at the MGF modified GCE, four separate peaks were obtained, possibly as a result of high surface area and excellent conductivity which MGF has. The Brunauer–Emmett–Teller (BET) surface area of the MGF was 2581 $m^2 g^{-1}$ [25], which was much larger than that of the common graphene nanosheets (466 $m^2 g^{-1}$) [28] and MWNTs (240.1 $m^2 g^{-1}$) [29]. With the large surface area, MGF could provide more active sites, so that the current was increasing significantly on MGF modified GCE. While compared with bare GCE, MWNTs/GCE and MGF/GCE, there were four increasing separate peaks appearing at MWNTs/MGF/GCE, indicating that the simultaneous determination of the four small biomolecules can be acheived at MWNTs/MGF modified GCE. This might be ascribed to synergy from the bridge of MWNTs to MGF, which made the surface area and conductivity increasing.

The impedance measurements of modified electrode in 0.1 mol L^{-1} PBS (pH=7.3) containing 5 mmol L^{-1} $[Fe(CN)_6]^{3-/4-}$ were proceeded to investigate the conductivity and electron transfer properties of different materials. The Nyquist plots for all electrodes are shown in Fig. 2B. As expected, after modification of MWNTs, GS MGF or MWNTs/MGF on the bare GCE, the plots exhibited much smaller semicircle in the high frequency region and the value of R_{ct} was decreased from 106 Ω (bare GCE) to 72 Ω (MWNTs) and 99 Ω (GS). The values of R_{ct} regarding to MGF and MWNTs/MGF were too small to obtain precisely for the error. The results indicated that the modified material can decrease the electron transfer resistance and improve the electron transfer process. By comparison, MWNTs/MGF possessed the minimum electron transfer resistance and its conductivity was the best. This was identical with the result of Fig. 2A.

Moreover, in order to investigate the effect of graphene obtained by different preparation methods, MWNTs/GS was modified on GCE. The DPV responses of 10 μmol L^{-1} DA, 100 μmol L^{-1} UA, 50 μmol L^{-1} TRP and 1 mmol L^{-1} AA at MWNTs/MGF/GCE and MWNTs/GS/GCE are shown in Fig. 3. Obviously, the peak currents for the four analytes were much larger on MWNTs/MGF/GCE than on MWNTs/GS/GCE, resulted from the difference of graphene. MGF obtained by using zeolite Ni-MCM-22 as catalyst and template possessed a large surface area and high conductivity owing to the special network structure avoid piling up the graphene sheets which can be seen from the SEM image. What is more, the network structure of MGF was better for the dispersion of MWNTs on the surface of MGF than GS, which may also improve the performance of the modified electrode.

To evaluate the peak separation, the redox behaviors of AA, DA, UA and TRP on MWNTs/MGF/GCE were investigated. For comparison, a bare GCE was used as control. The cyclic voltammograms of

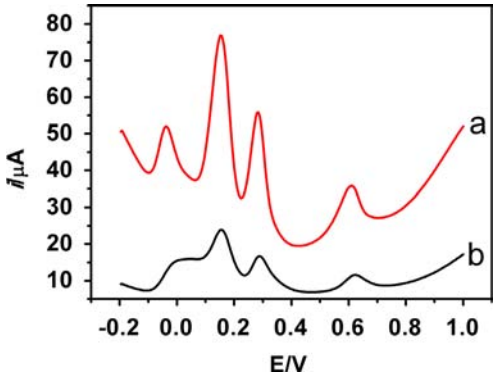

Fig. 3. DPVs of MWNTs/MGF/GCE (a) and MWNTs/GS/GCE (b) in 0.10 mol L^{-1} PBS (pH 7.3) containing 10 μmol L^{-1} DA, 100 μmol L^{-1} UA, 50 μmol L^{-1} TRP and 1.0 mmol L^{-1} AA, respectively.

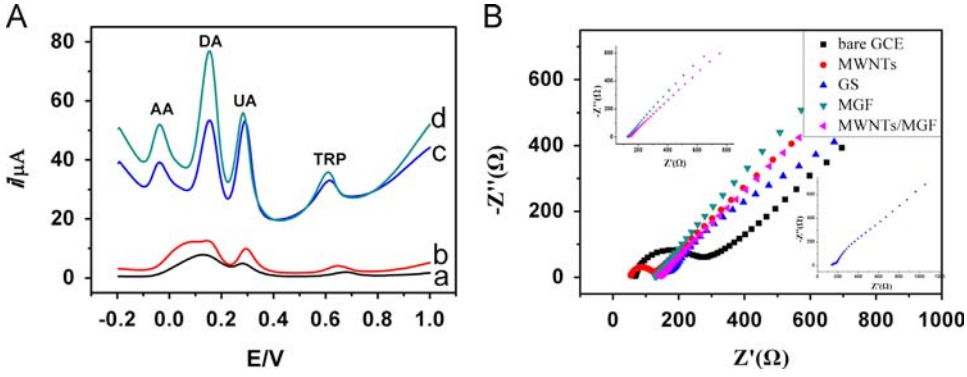

Fig. 2. (A) DPVs of GCE (a), MWNTs/GCE (b), MGF/GCE (c) and MWNTs/MGF/GCE (d) in 0.10 mol L^{-1} PBS (pH 7.3) containing 10 μmol L^{-1} DA, 100 μmol L^{-1} UA, 50 μmol L^{-1} TRP and 1 mmol L^{-1} AA, respectively. (B) The Nyquist plots of modified electrode in 0.1 mol L^{-1} PBS (pH=7.3) containing 5 mmol L^{-1} $[Fe(CN)_6]^{3-/4-}$.

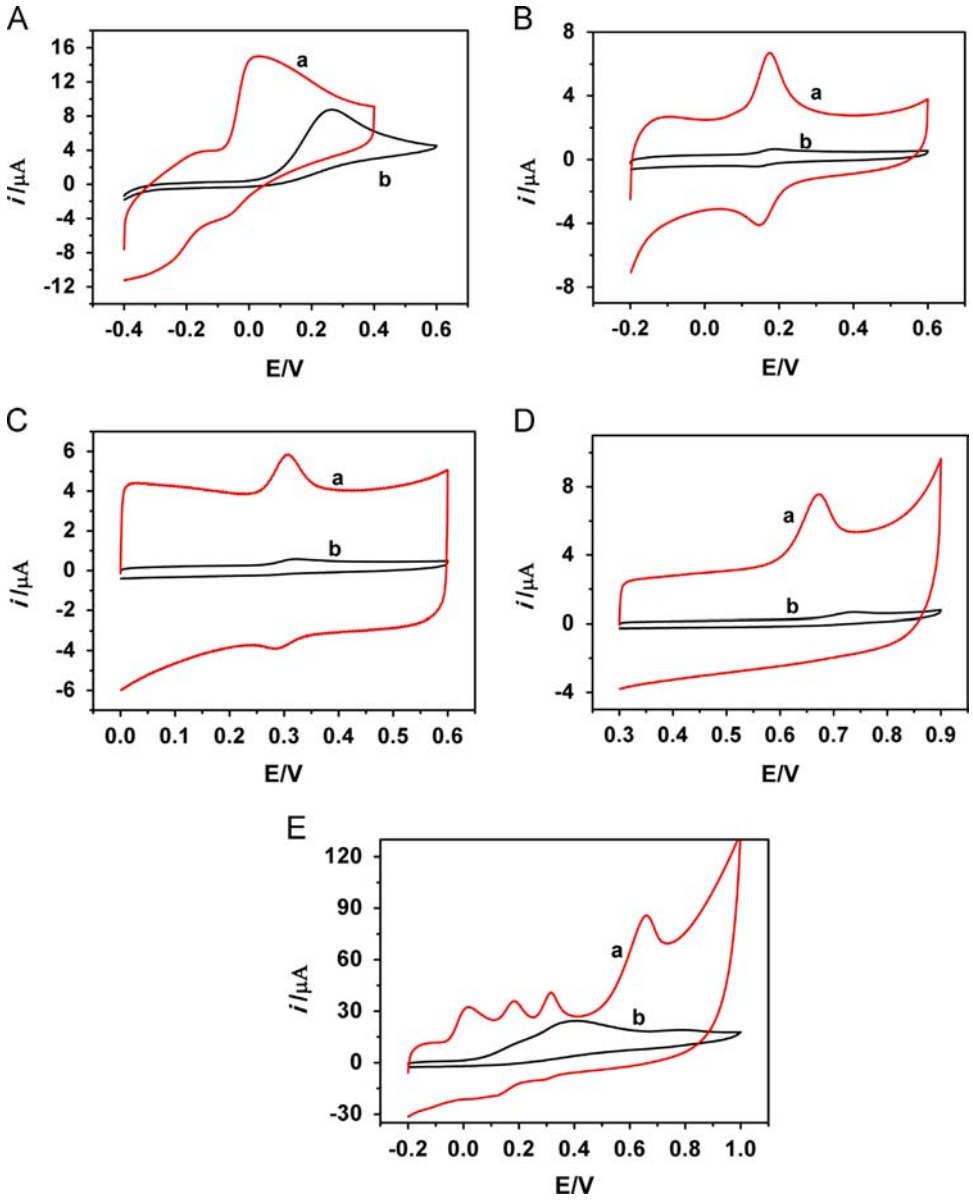

Fig. 4. Cyclic voltammograms of 1.0 mmol L^{-1} AA (A), 10 μmol L^{-1} DA (B), 10 μmol L^{-1} UA (C), and 10 μmol L^{-1} TRP (D) at MWNTs/MGF/GCE (curve a) and bare GCE (curve b) in 0.10 mol L^{-1} PBS (pH 7.3). (D) shows the cyclic voltammograms of 0.10 mol L^{-1} PBS (pH 7.3) containing 1.0 mmol L^{-1} AA, 10 μmol L^{-1} DA, 100 μmol L^{-1} UA and 50 μmol L^{-1} TRP. The scan rate was 50 mV s^{-1}.

Table 1
The oxidation peak currents and peak potentials of four analytes on bare GCE and modified electrode.

Analyte	i_{pa} (μA)		E_{pa} (V)	
	Bare GCE	MWNTs/MGF/GCE	Bare GCE	MWNTs/MGF/GCE
AA	6.814	10.76↑	0.265	0.034↓
DA	0.307	4.211↑	0.188	0.175↓
UA	0.291	1.989↑	0.326	0.307↓
TRP	0.377	4.067↑	0.736	0.672↓

these four analytes on the bare and MWNTs/MGF/GCE are shown in Fig. 4. The information obtained from Fig. 4 is generalized in Table 1, through which we can see that the oxidation peak currents were increasing and the oxidation peak potentials were shifted negatively on MWNTs/MGF/GCE compared to bare GCE. This indicates that the electron transfer kinetics of the analytes were faster on modified electrode than bare GCE. On MWNTs/MGF/GCE, the peak potential of AA was negatively shifted to 231 mV, while the potential of DA was negatively shifted only to 13 mV. Different shift degrees of AA and DA made the peaks separated from one broad and mixed peak.

3.3. Optimization of ratio of MWNTs to MGF

In order to seek for the optimal ratio of MWNTs to MGF, the ratio of MWNTs to MGF was changed from 3:1 to 1:3, as shown in Fig. 5. Every peak current increases with the increase of the amount of MGF. Until the ratio of MWNTs to MGF was 1, peak currents reached to maximum, and there was no apparent change with the further increase of MGF. So the optimal ratio of MWNTs to MGF was 1:1 and following experiments were carried out at this ratio.

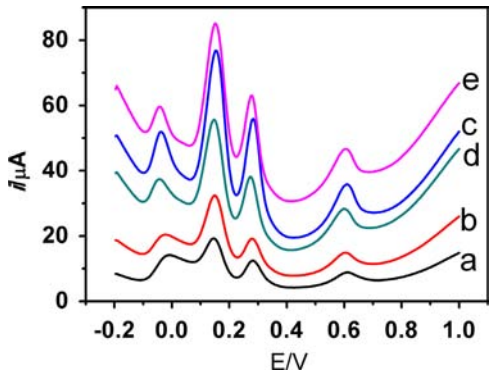

Fig. 5. DPVs of GCE modified with different ratios of MWNTs/MGF (3/1, 2/1, 1/1, 1/2, and 1/3 for a–e) in 0.10 mol L^{-1} PBS (pH 7.3) containing 10 μmol L^{-1} DA, 100 μmol L^{-1} UA, 50 μmol L^{-1} TRP and 1.0 mmol L^{-1} AA, respectively.

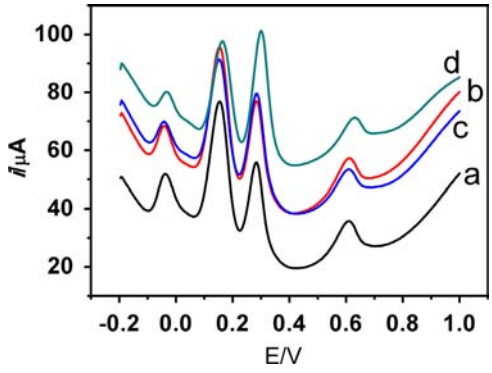

Fig. 6. DPVs of GCE modified with different amount of MWNTs/MGF nanocomposite (1–4 μL for a–d) in 0.10 mol L^{-1} PBS (pH 7.3) containing 10 μmol L^{-1} DA, 100 μmol L^{-1} UA, 50 μmol L^{-1} TRP and 1.0 mmol L^{-1} AA, respectively.

3.4. Optimization of amount of MWNTs/MGF modified on GCE

The effects of the amount of MWNTs/MGF nanocomposite on the DPV responses of the modified GCE in 0.10 M PBS (pH 7.3) containing 10 μmol L^{-1} DA, 100 μmol L^{-1} UA, 50 μmol L^{-1} TRP and 1 mmol L^{-1} AA are examined in Fig. 6. With the amount increasing from 1 μL to 4 μL, all peak current responses were found with no increase or tiny decrease. This may be because the surface area of MWNTs/MGF nanomaterial was large enough, so that with only little amount, four analytes can be effectively and simultaneously detected. Hence, 1 μL MWNTs/MGF was chosen as the best amount for modification on GCE.

3.5. Influence of pH

The effect of pH of the supporting electrolyte solution on the DPV response of the four analytes is tested in Fig. 7. As the pH of body fluid is around neutral, the neutral and neighboring pH (5.0, 7.3 and 9.3) was chosen to compare in this experiment. With the increasing of pH value, all the peak potentials of AA, DA, UA and TRP shifted, indicating that protons involved in the oxidation processes [21] When the pH value was 5.0, peak currents were small. While peak currents doubled with the pH increased to 7.3. When the pH increased continuously to 9.3, current responses remained similarly with that at pH 7.3 except that the peak attributed to UA was so close to the peak of DA that the determination of UA was disturbed. As a result, the optimal pH of the supporting electrolyte solution was 7.3, which was also in accordance with the pH of body fluid.

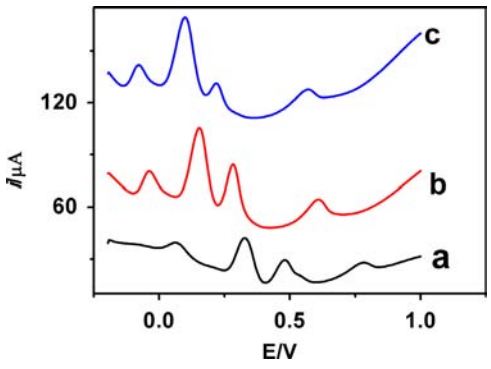

Fig. 7. Influence of pH of the supporting electrolyte (0.10 mol L^{-1} PBS) on DPV detection to 10 μmol L^{-1} DA, 100 μmol L^{-1} UA, 50 μmol L^{-1} TRP and 1.0 mmol L^{-1} AA at MWNTs/MGF/GCE. a: pH 5.0; b: pH 7.3; c: pH 9.3.

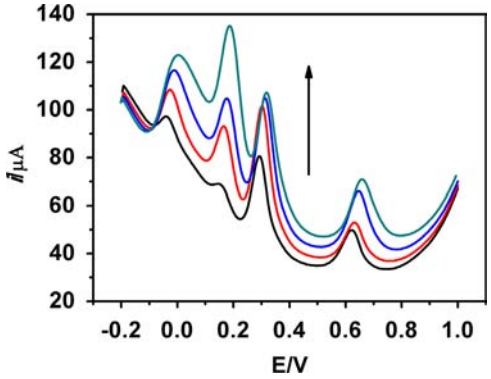

Fig. 8. DPVs of simultaneous determination of AA, DA, UA and TRP using MWNTs/MGF modified GCE in 0.1 mol L^{-1} PBS (pH 7.3). Concentrations of the four compounds: AA (0.5, 1, 3, 6, and 10) mmol L^{-1}; DA (0.6, 1, 5, 10, and 50) μmol L^{-1}; UA (50, 100, 300, 500, and 800) mmol L^{-1} and TRP (30, 60, 100, 300, and 500) μmol L^{-1}.

3.6. Simultaneous detection of AA, DA, UA and TRP

Fig. 8 demonstrates the DPV curves of various AA, DA, UA and TRP concentrations in the mixture solution at MWNTs/MGF/GCE. Under the optimal conditions, the peaks of AA, DA, UA and TRP were separated clearly, and the peak currents increased with the increase of concentrations of four analytes. Hence, the simultaneous detection of AA, DA, UA and TRP in the mixture solution was possible.

As mentioned, AA, DA, UA and TRP usually coexist in biological matrixes. So it is important to selectively determine these small molecules in a mixture solution. Fig. 9 shows the DPV responses of AA, DA, UA and TRP in a mixture in which the concentration of one substance changed, while the other three species remained constant. Under such condition, the peak current of this substance increased linearly with increase in its concentration in certain scope. The detailed results are shown in Table 2. What is more, the performance of this modified electrode compared with those modified with other nanomaterials reported previously is shown in Table 3. The results showed that MWNTs/MGF/GCE possessed satisfactory linear range and detection limit for the simultaneous detection of AA, DA, UA and TRP.

3.7. Interferences, reproducibility and stability

The ability of anti-interference of the modified electrode was also investigated. Results indicate that no significant interference on the detection of 1 mmol L^{-1} AA, 10 μmol L^{-1} DA, 100 μmol L^{-1}

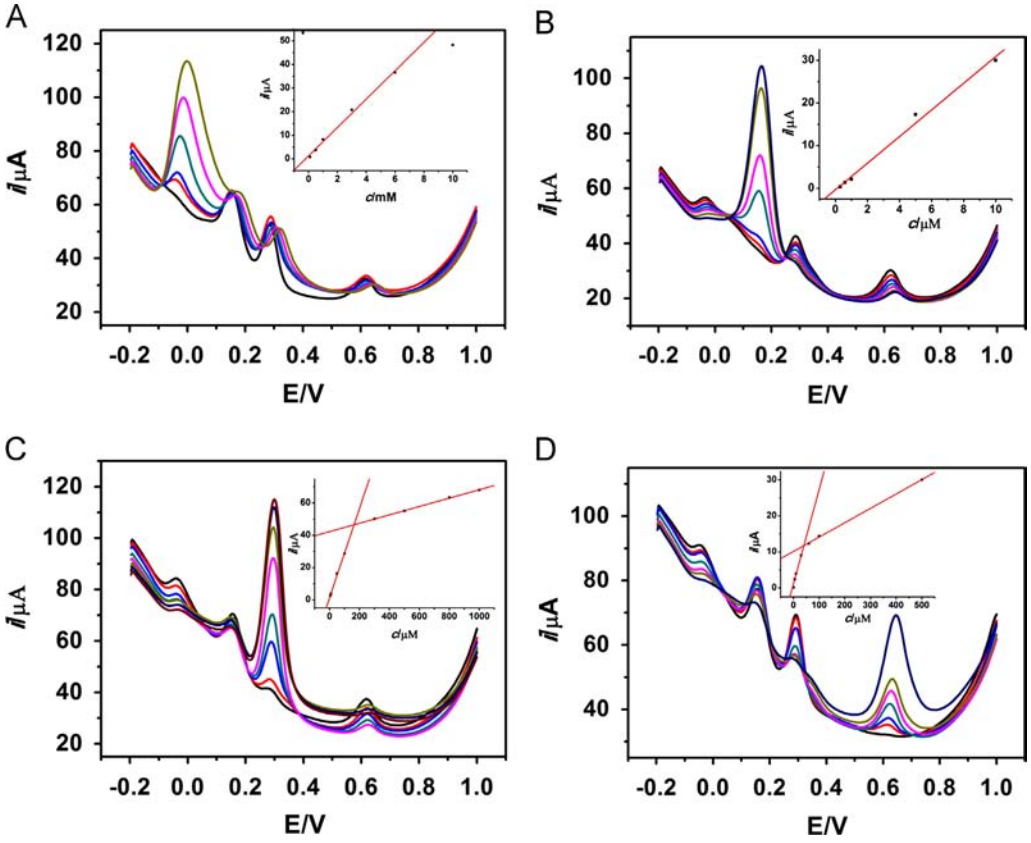

Fig. 9. DPVs at the MWNTs/MGF/GCE in 0.1 mol L^{-1} (pH 7.3). (A) containing 2 μmol L^{-1} DA, 50 μmol L^{-1} UA, 20 μmol L^{-1} TRP and different concentrations of AA (from inner to outer): 0.1, 0.5, 1, 3, 6, and 10 mmol L^{-1}; (B) containing 0.5 mmol L^{-1} AA, 50 μmol L^{-1} UA, 50 μmol · L^{-1} TRP and different concentrations of DA (from inner to outer): 0.3, 0.6, 1, 5, 10, 30, and 50 μmol L^{-1}; (C) containing 0.5 mmol L^{-1} AA, 2 μmol L^{-1} DA, 20 μmol L^{-1} TRP and different concentrations of UA (from inner to outer): 5, 10, 50, 100, 300, 500, 800, and 1000 μmol L^{-1}; (D) containing 0.5 mmol L^{-1} AA, 2 μmol L^{-1} DA, 30 μmol L^{-1} UA and different concentrations of TRP (from inner to outer): 1, 5, 10, 30, 60, 100, and 500 μmol L^{-1}.

Table 2
The linear response range, linear regression equation and detection limit of one analyte in a mixture of three other analytes coexisting.

Analyte	Linear response range (μmol L^{-1})	Linear regression equation	Detection limit (μmol L^{-1}) ($S/N=3$)
AA	100–6000	i_{AA} (μA) = 1.2883 + 6.01932C (μmol L^{-1}) (r=0.992)	18.28
DA	0.3–10	i_{DA} (μA) = −0.32943 + 3.11875C (μmol L^{-1}) (r=0.989)	0.06
UA	5–100	i_{UA} (μA) = 1.45424 + 0.27641C (μmol L^{-1}) (r=0.995)	0.93
	300–1000	i_{UA} (μA) = 42.2981 + 0.02594C (μmol L^{-1}) (r=0.998)	
TRP	5–30	i_{TRP} (μA) = 1.21226 + 0.26187C (μmol L^{-1}) (r=0.997)	0.87
	60–500	i_{TRP} (μA) = 10.15417 + 0.03988C (μmol L^{-1}) (r=0.998)	

Table 3
Comparison of analytical performance of GCE modified with MWNTs/MGF or other nanomaterials reported previously.

Modified electrode	Linear response range (μmol L^{-1})				Limit of detection (μmol L^{-1})				References
	AA	DA	UA	TRP	AA	DA	UA	TRP	
GS–PTCA	20–420	0.4–370	4–540	0.4–140	5.60	0.13	0.92	0.06	[13]
Fe(III)P/MWCNTs	14–2500	0.7–3600	5.8–1300	–	3.00	0.09	0.30	–	[19]
GNPs/PImox	210.0–1010.0	5.0–268.0	6.0–486.0	3.0–34.0 84.0–464.0	2.0	0.08	0.5	0.7	[16]
MWCNT–FeNAZ-CH	7.77–833	7.35–833	0.23–83.3	0.074–34.5	1.11	1.05	0.033	0.011	[17]
Graphene	–	4–100	–	–	–	2.64	–	–	[30]
MWNTs/MGF	100–6000	0.3–10	5–100 300–1000	5–30 60–500	18.28	0.06	0.93	0.87	This work

GS–PTCA: hybrid of graphene sheets (GS) and 3, 4, 9, 10-perylenetetracarboxylic acid (PTCA); Fe(III)P/MWCNTs: chloro [3,7,12,17-tetramethyl-8,13-divinylporphyrin-2,18-dipropanoato (2−)]iron(III)/multi-walled carbon nanotubes; GNPs/PImox: gold nanoparticles/overoxidized-polyimidazole composite; MWCNT–FeNAZ-CH: iron ion-doped natrolite zeolite–multiwalled carbon nanotube.

UA and 50 μmol L^{-1} TRP was observed for common substances: Na^+, K^+, Ca^{2+}, Mg^{2+} and glucose. The stability of the prepared electrode was examined by using the same MWNTs/MGF/GCE for 5 repetitive measurements in the same solution containing 1 mmol L^{-1} AA, 10 μmol L^{-1} DA, 100 μmol L^{-1} UA and 50 μmol L^{-1} TRP. The relative standard deviation (RSD) for all these substances

was less than 6.5%, confirming that the modified electrode for determination of AA, DA, UA and TRP was stable. The modified electrode was stored at room temperature when it was not in use. The response of the electrode remains 91%, 96%, 93% and 89% for AA, DA, UA and TRP of its initial value after 2 weeks. These results implied that the proposed electrode possessed good stability.

4. Conclusions

In this work, a MWNTs/MGF modified GCE was successfully constructed and employed for the simultaneous determination of AA, DA, UA and TRP. The modified electrode exhibited high sensitivity and selectivity towards the oxidation of AA, DA, UA and TRP, and resolved the overlapped oxidation peaks of AA, UA and TRP into three well-defined peaks respectively. This was attributed to the large surface areas and high conductivity which MWNTs/MGF nanocomposite possessed. The DPV responses to AA, DA, UA and TRP were linear with the concentrations over a wild range. The present strategy provides a novel and promising platform for the simultaneous determination of AA, DA, UA and TRP in human metabolism.

Acknowledgments

This work was supported by the National Natural Science Foundation of China (21175029, 11074053 and 31170802) and the Shanghai Leading Academic Discipline Project (B109).

References

[1] S.J. Yu, C.H. Luo, L.W. Wang, H. Peng, Z.Q. Zhu, Analyst 138 (2013) 1149–1155.
[2] J. Arguello, V.L. Leidens, H.A. Magosso, R.R. Ramos, Y. Gushikem, Electrochim. Acta 54 (2008) 560–565.
[3] X.Q. Tian, C.M. Cheng, H.Y. Yuan, J. Du, D. Xiao, S.P. Xie, M.M.F. Choi, Talanta 93 (2012) 79–85.
[4] O. Arrigoni, M.C. De Tullio, Biochim. Biophys. Acta Gen. Subj. 1569 (2002) 1–9.
[5] J.R. Delanghe, M.R. Langlois, M.L. De Buyzere, N. Na, J. Ouyang, M. M. Speeckaert, M.A. Torck, Genes Nutr. 6 (2011) 341–346.
[6] S.R. Ali, Y.F. Ma, R.R. Parajuli, Y. Balogun, W.Y.C. Lai, H.X. He, Anal. Chem. 79 (2007) 2583–2587.
[7] Y.Z. Zhou, H.Y. Zhang, H.D. Xie, B. Chen, L. Zhang, X.H. Zheng, P. Jia, Electrochim. Acta 75 (2012) 360–365.
[8] A.A. Ensafi, A. Arabzadeh, H. Karimi-Maleh, Anal. Lett. 43 (2010) 1976–1988.
[9] Y. Xue, H. Zhao, Z.J. Wu, X.J. Li, Y.J. He, Z.B. Yuan, Biosens. Bioelectron. 29 (2011) 102–108.
[10] X.L. Niu, W. Yang, H. Guo, J. Ren, F.S. Yang, J.Z. Gao, Talanta 99 (2012) 984–988.
[11] D.X. Ye, L.Q. Luo, Y.P. Ding, B.D. Liu, X. Liu, Analyst 137 (2012) 2840–2845.
[12] C.X. Xu, K.J. Huang, Y. Fan, Z.W. Wu, J. Li, T. Can, Mater. Sci. Eng. C Mater. Biol. Appl. 32 (2012) 969–974.
[13] W. Zhang, Y.Q. Chai, R. Yuan, S.H. Chen, J. Han, D.H. Yuan, Anal. Chim. Acta 756 (2012) 7–12.
[14] D.G. Patrascu, V. David, I. Balan, A. Ciobanu, I.G. David, P. Lazar, I. Ciurea, I. Stamatin, A.A. Ciucu, Anal. Lett. 43 (2010) 1100–1110.
[15] Z.Q. Gao, H. Huang, Chem. Commun. (1998) 2107–2108.
[16] C. Wang, R. Yuan, Y.Q. Chai, S.H. Chen, F.X. Hu, M.H. Zhang, Anal. Chim. Acta 741 (2012) 15–20.
[17] M. Noroozifar, M. Khorasani-Motlagh, R. Akbari, M.B. Parizi, Biosens. Bioelectron. 28 (2011) 56–63.
[18] W. Zhang, R. Yuan, Y.Q. Chai, Y. Zhang, S.H. Chen, Sens. Actuator B Chem. 166 (2012) 601–607.
[19] C. Wang, R. Yuan, Y.Q. Chai, S.H. Chen, Y. Zhang, F.X. Hu, M.H. Zhang, Electrochim. Acta 62 (2012) 109–115.
[20] L. Zhang, Z.G. Shi, Q.H. Lang, J. Solid State Electrochem. 15 (2011) 801–809.
[21] B. Habibi, M.H. Pournaghi-Azar, Electrochim. Acta 55 (2010) 5492–5498.
[22] S. Palanisamy, S.H. Ku, S.M. Chen, Microchim. Acta 180 (2013) 1037–1042.
[23] X.L. Niu, W. Yang, H. Guo, J. Ren, J.Z. Gao, Biosens. Bioelectron. 41 (2013) 225–231.
[24] K.S. Novoselov, A.K. Geim, S.V. Morozov, D. Jiang, Y. Zhang, S.V. Dubonos, I.V. Grigorieva, A.A. Firsov, Science 306 (2004) 666–669.
[25] Y. Wang, H.X. Li, J.L. Kong, Sens. Actuator B Chem. 193 (2014) 708–714.
[26] D.X. Ye, L.Q. Luo, Y.P. Ding, Q. Chen, X. Liu, Analyst 136 (2011) 4563–4569.
[27] X.L. Xu, F. Huang, G.L. Zhou, S. Zhang, J.L. Kong, Sensors 10 (2010) 8398–8410.
[28] S. Stankovich, D.A. Dikin, R.D. Piner, K.A. Kohlhaas, A. Kleinhammes, Y. Jia, Y. Wu, S.T. Nguyen, R.S. Ruoff, Carbon 45 (2007) 1558–1565.
[29] F.X. Li, Y. Wang, D.Z. Wang, F. Wei, Carbon 42 (2004) 2375–2383.
[30] Y.R. Kim, S. Bong, Y.J. Kang, Y. Yang, R.K. Mahajan, J.S. Kim, H. Kim, Biosens. Bioelectron. 25 (2010) 2366–2369.